Desalination and Water Treatment
www.deswater.com

doi:10.5004/dwt.2017.21477

93 (2017) 61–73
October

Sewage sludge-based activated carbon: its application for hexavalent chromium from synthetic and electroplating wastewater in batch and fixed-bed column adsorption

Zohreh Aliakbari[a], Habibollah Younesi[a,*], Ali Asghar Ghoreyshi[b], Nader Bahramifar[a], Ava Heidari[c]

[a]*Department of Environmental Science, Faculty of Natural Resources, Tarbiat Modares University, Imam Reza Street, Noor, P.O. Box: 4641776489, Iran, Tel. +98 1155443101, Fax +98 11 55443499, email: hunesi@modares.ac.ir, hunesi@yahoo.com*
[b]*Department of Chemical Engineering, Babol University of Technology, Babol, Iran*
[c]*Natural Resources and Environment College, Ferdowsi University of Mashhad, Mashhad, Iran*

Received 17 January 2017; Accepted 22 September 2017

ABSTRACT

As-prepared activated carbons (ACs) were utilized as an adsorbent for removal of Cr (VI) ions from aqueous solution. The effects of different operating parameters such as adsorbent dosage, pH, contact time, initial Cr (VI) concentration and temperature were conducted by batch experiments. According to experimental results, the equilibrium time, the optimum pH, and adsorbent dosage were found 120 min, pH 3, 5 g/l, respectively, with 2.5 g H_3PO_4 of carbonized sample and post-treatment step by refluxing with HCl and NaOH and autoclaved with HF (arAC) with the BET surface area of 472 mg/g. The equilibrium adsorption data were fitted well by Langmuir and Freundlich adsorption model with a monolayer maximum adsorption capacity of 12.8 mg/g. The rate of Cr (VI) adsorption onto the AC was reasonably explained by the pseudo-second-order kinetic model. In addition, the thermodynamic parameters of the adsorption process such as standard Gibb's free energy (ΔG°), standard enthalpy (ΔH°) and standard entropy (ΔS°) were evaluated. In a fixed-bed column adsorption, the effects of bed height, flow rate and initial ion concentration on the breakthrough curve were investigated, on which the predictions were found to be satisfactory both by the Yan models. The results showed that a maximum of adsorption capacity was 94.54 $mg.g^{-1}$ by the sample of the arAC. Finally, we found out the sewage sludge-based AC was an efficient low-cost adsorbent for Cr (VI) removal from electroplating industrial wastewater.

Keywords: Activated carbon; Sewage sludge; Chromium;Batch and fixed-bed column

1. Introduction

Heavy metal ion contamination of water is a very serious environmental problem all over the world. Chromium (Cr) is one of the heavy metals that are often found in water and wastewater. Cr (VI) compounds are more of a concern than Cr (III) due to their toxicity. The presence of Cr (VI) in the wastewaters is toxic and has a harmful influence on the living organisms in the water and on the human health. Health problems caused by Cr (VI) include nausea, diarrhea, skin rashes, respiratory problems, liver and kidney damage, internal hemorrhaging and lung cancer [1]. Despite their toxicity, the chromium compounds are widely used in dyes and paints, tanning of leather, metal finishing, electroplating, and so on. Conventional methods for the removal of the metal ions from the wastewater are chemical precipitation, chemical oxidation and reduction, ion exchange, filtration, electrochemical treatment and evaporative recovery. However, these technological processes have significant drawbacks, including imperfect metal removal, the need for expensive equipment and monitoring systems, high reagent and energy requirements, production of toxic sludge and disposal problem [2]. Adsorption has become

*Corresponding author.

one of the alternative treatment techniques for wastewater containing heavy metals. Several adsorbents such as AC [3], clay materials [4], carbon nanotube [5], metal oxides, and zeolite [6] can be used for removal of metal ions from wastewater.

The production of AC from municipal and wastewater sewage sludge has been reported in previous studies. Smith et al. [7] reviewed the published research on production, properties, and application of sewage sludge-based AC. There is a lack of information about the detailed studies of the process parameters, the kinetics and the thermodynamics of Cr (VI) adsorption onto AC-based municipal sewage sludge in the literature. The influence of the type of post-treatment of AC with HCl and NaOH on the removal of Cr (VI) from aqueous solution was investigated for the first time in the present study.

In this study, the AC was prepared from municipal sewage sludge by chemical activation by H_3PO_4 at 450°C at different impregnation ratio. The effects of different H_3PO_4 activating agent amounts and post-treatment purification methods were studied to optimize pore size distribution and surface area of AC. The influence of multiple operating parameters for adsorption of Cr (VI), such as contact time, initial concentration, temperature, pH, and the adsorbent dose was investigated in batch systems. The adsorption kinetic, isotherm and thermodynamic were also discussed.

2. Material and methods

2.1. Electroplating wastewater characteristics

The effluent samples of the local electroplating industry (Sari, Mazandaran, Iran) from chrome plating units were collected. The sample was analyzed for color, pH, total dissolved solid (TDS), chemical oxygen demand (COD), biochemical oxygen demand (BOD), Cr (VI) concentration. All analyses were performed in accordance with standard methods for the examination of water and wastewater [8] and the average values and standard deviation (SD) of characteristics are presented in Table 1. The Cr (VI) removal efficiency of as-produced AC for electroplating wastewater was examined. Then, the sample was brought into contact with ACs into a fixed-bed column at room temperature of 25°C and pH 3 with column bed height of 20 mm and flow rate of 1 ml/min. The residual Cr (VI) concentration was read in the samples using AAS.

Table 1
Characteristics of wastewater from electroplating industry

Characteristic	Average value ± SD
pH	6.6 ± 0.33
Cr (VI) concentration, mg/l	148 ± 7.5
COD, mg/l	223 ± 11.7
BOD_5, mg/l	60 ± 4
TKN, mg/l	0.004386 ± 0.0021
TSS, mg/l	–
TDS, mg/l	2118 ± 110
VSS, mg/l	–
EC, dS/m	129.94 ± 6.24

2.2. Activated carbon preparation

In our previous study [9], we evaluated different preparation processes of the activated carbon from sewage sludge in three different strategies for synthesizing five different ACs and comprised carbonization, post-treatment purification methods for removing the inorganic fractions of the carbonaceous framework. The study was involved different strategy of preparation and characterization only. However, The FTIR spectra of prepared ACs from sewage sludge showed different functional groups onto ACs surface, the most abundant functional groups found onto the prepared ACs include carboxylic acid (C–O and O–H stretching mode), aromatic (C–H and C–C stretching mode), carbonyl (C=O stretching mode) and alkane (C–H stretching and bending modes). It was found that the maximum specific surface area of AC treated with sodium hydroxide (bsAC) was 635 m^2/g. As prepared ACs in powders form were less than 1.0 mm in size with an average diameter between 0.1 and 0.2 mm and 95–100% of which were passed through an 80-mesh sieve (0.177 mm). Table 2 shows the characteristic of adsorbents used in the present study. In the present study, its application for Cr (VI) removal from electroplating wastewater was carried out in batch and fixed-bed column adsorption.

2.3. Batch adsorption experiment

A stock solution of 1000 mg/l of Cr (VI) was prepared by dissolving 2.829 g potassium dichromate salt ($K_2Cr_2O_7$, Aldrich, USA) in 1000 ml deionized water. This solution was diluted with deionized water to obtain the desired Cr (VI) concentration for adsorption experiment. The batch adsorption test was used to investigate the influence of the contact time, pH, dosage, initial Cr (VI) concentration and temperature on the adsorption capacity of the AC. After desired contact time, the suspension was filtered with 0.45 µm syringe filter in order to remove the AC adsorbent and the concentration of Cr (VI) in the filtrate was measured using atomic absorption spectrophotometer (AAS, PU 9400 X, Philips Scientific, Cambridge, UK). The effect of pH, in the range of 2–7, on adsorption of Cr (VI) by AC was investigated. The initial pH of the solution was adjusted using required amount of 0.1 M HCl or 0.1 M NaOH solution. For Cr (VI) adsorption, a known amount of AC (0.4 g) was suspended in 100 ml solution containing 50 mg/l of Cr (VI) in an Erlenmeyer flask. The flask was agitated on a magnetic stirrer (200 rpm) for 120 min at room temperature (25°C). The concentration of Cr (VI) ions remained in the aqueous phase at equilibrium was measured. After the optimum pH value was obtained, the effect of dose of AC was investigated. The effect of dosage on adsorption of Cr (VI) by AC was studied by the addition of different adsorbent dosage (2, 3, 4 and 5 g/L) in 250-ml Erlenmeyer flasks containing 100 ml aqueous solution of 50 mg/l at pH 3.The batch adsorption isotherm experiment as made known in the examination of the effect of different initial Cr (VI) concentration. The values of Cr (VI) concentration investigated

Table 2
Properties of as-synthesized activated carbon

Carbon materials	$AC_{HP2.5}$	arAC	brAC	haAC	bsAC
Porosity	Mesopore	Mesopore	Mesopore	Mesopore	Mesopore
Total pore volume, cm^3/g	0.060	0.573	0.616	0.608	0.496
BET surface area, m^2/g	19.59	472	432	511	635
Bed density, kg/m^3	25 to 26				
Prosity (ε)	~0.15				

were 10, 30, 50, 70, 110 mg/l. The suspension was agitated on a magnetic stirrer in 250-ml Erlenmeyer flasks containing 100 ml metal ion solution at pH 3, AC dosage of 4 g/land room temperature. The samples were withdrawn at specified intervals of time, filtered and the supernatant was analyzed to measure the Cr (VI) concentration. The study temperature effect on the adsorption capacity of the AC for Cr (VI) was evaluated at three temperatures (25, 35 and 45°C), 4 g/l adsorbent dosage, pH 3, 120 min contact time and 50 mg/l initial Cr (VI) concentration.

2.4. Fixed-bed column experiments

In order to analyze the adsorption capability of ACs, dynamic removal of Cr (VI) ion from aqueous solution was conducted in a vertical cylindrical glass tube of 5 mm inner diameter (ID) and 20 cm effective height. The column was packed with sewage sludge-based AC between two supporting layers of glass wool and was operated in an up flow mode using a peristaltic pump (pump drive 5101, Heidolph, Germany). The Cr (VI) ion concentration was determined by collecting solution samples at regular time intervals at the sampling ports near the inlet and outlet of the column. The experiments were carried out as a function of different bed height (20, 40 and 60 mm) of, influent flow rates (0.5, 1 and 1.5 ml/min) and initial Cr (VI) ion concentrations (20, 40 and 60 mg/l) and at pH 3 and room temperature. The saturation of the column was detected by measuring the concentration of Cr (VI) in the fluid phase at the outlet of the column.

2.5. Isotherm, kinetic and thermodynamic of Cr (VI) adsorption on AC

The adsorption capacity and percentage removal efficiency of AC were calculated by the following equations:

$$q_e = \frac{C_0 V_0 - C_e V_e}{m} \tag{1}$$

$$R = \frac{C_o - C_t}{C_o} \times 100 \tag{2}$$

where C_o and C_e are the initial and the equilibrium Cr (VI) concentration, respectively (mg/l), V the volume of the solution (l) and m the mass of the adsorbent (g).

The Langmuir and Freundlich adsorption isotherms were used to describe the adsorption of Cr (VI) from aqueous solute ion. Langmuir model supposes that uptake of adsorbate molecules occurs on a homogenous surface by monolayer without interaction between adsorbed molecules, moreover, this model assumes uniform energy of adsorption onto the adsorbent surface and no transmigration of the adsorbate [10,11]. The nonlinear form of the Langmuir and Freundlich equations are given as follows [12,13]:

$$q_e = \frac{K q_m C_e}{1 + K C_e} \tag{3}$$

where C_e is the equilibrium Cr (VI) concentration (mg/l), q_e the amount of Cr (VI) adsorbed on adsorbent at equilibrium (mg/g), q_m the maximum adsorption capacity (mg/g) and K the Langmuir constants (l/mg), indicating the binding energy of adsorption. The Freundlich isotherm suggests a multilayer adsorption system in which adsorption takes place on the heterogeneous energetic active sites on the surface with the interaction between adsorbed molecules. This can be due to heterogeneous oxygen groups, such as carbonyl, phenolic, and lactone functional groups, on the AC [11]:

$$q_e = K_f C_e^{\frac{1}{n}} \tag{4}$$

where K_f and n are Freundlich constants which are related to the Cr (VI) adsorption capacity and the adsorption intensity, respectively.

The simple kinetic model that expresses adsorption mechanism is pseudo-first order as suggested by Lagergren [14,15], which can be defined by Eq. (5):

$$\frac{dq_t}{dt} = k_1 \left(q_e - q_t \right) \tag{5}$$

where k_1 is the first-order rate constant (min^{-1}), q_e and q_t are the amounts of Cr (VI) adsorbed on adsorbent (mg/g) at equilibrium and at time t (min), respectively. Integrating and using the boundary condition, $t = 0$ and $q_t = 0$ to $t = t$ and $q_e = q_t$ gives the form:

$$\log\left(q_e - q_t \right) = \log q_e - \frac{K_1}{2.303} t \tag{6}$$

The Cr (VI) adsorption kinetics may be matched by a pseudo-second-order model. The linear form of this model is given by the following equation:

$$\frac{t}{q_t} = \frac{1}{k_2 q_e^2} + \frac{1}{q_e} t \tag{7}$$

where k_2 (g/mg/min) is pseudo-second-order rate constant. Value k_2 and q_e can be determined from the slope and the intercept of the plot t/q_t against t,respectively.

The thermodynamic parameters such as free energy change (ΔG°) for the adsorption of Cr (VI) onto AC was calculated using the following equations [12,16]:

$$\Delta G'' = -RTlnK_d \tag{8}$$

$$K_d = \frac{q_e}{C_e} \tag{9}$$

where ΔG° is the change in free energy (kJ/mol), T the temperature (K), R the gas constant (8.314 J/mol·K), K_d the equilibrium constant of adsorption (l/g), q_e the amount adsorbed on adsorbent at equilibrium and C_e is the equilibrium concentration. The change in the standard enthalpy (ΔH°, kJ/mol) and the change in the standard entropy (ΔS°, J/mol·K) can be evaluated using the following equation [12,16]:

$$\Delta G^o = \Delta H^o - T\Delta S^o \tag{10}$$

The Van't Hoff equation can be used to estimate the variation of the equilibrium constant with temperature. The combined form of the Eqs. (8) and (10) is given as:

$$\ln K_d = \frac{\Delta S}{R} - \frac{\Delta H}{RT} \tag{11}$$

The standard enthalpy and entropy changes were obtained from the slope and intercept of a plot with ln K_d on the y-axis and $1/T$ on the x-axis, respectively.

The rate constant of pseudo-second-order kinetic increased with increasing temperature. The dependence of kinetic rate constant of an adsorption on temperature can be stated by the Arrhenius equation as follows:

$$q_{total} = \frac{QC_o}{1000}\int_{t=0}^{t=t_{total}}\left(1-\frac{C_t}{C_0}\right)dt \tag{12}$$

where, E_a is the activation energy of the adsorption in kJ/mol, R the gas constant in 8.314 J mol^{-1} K^{-1}, T the temperature in K and A represents the collision frequency, which is called the frequency factor.

2.6. Fixed-bed column data analysis and modeling

In the fixed-bed adsorption, the variety of concentrations in the fluid phase and solid phase as a function of time as well as with position in the bed is called a breakthrough curve. The abrupt rise in the concentration of the adsorbate in the effluent (C_t) reaches about 5% of the influent concentration (C_o), indicating the breakthrough time (t_b). The column experiment is carried out to the complete saturation point of the adsorbent bed, i.e., when the concentration of the adsorbate in the effluent reaches 95% of the influent concentration, indicating exhausting time (t_e). From a mass balance in the column, the area under the breakthrough curve represents the total mass of metal adsorbed (q_{total}, mg) and can be obtained by the following equation:

$$q_{total} = \frac{QC_o}{1000}\int_{t=0}^{t=t_{total}}\left(1-\frac{C_t}{C_0}\right)dt \tag{13}$$

where q_{total} is the total metal ions run through a column (mg), C_o the feed concentration of metal ion (mg/l), Q the volumetric flow rate (ml/min) and C_t the concentration of metal ion at the outlet of the column (mg/l). The total amount of metal ion (mg) passed through the column and the percentage removal of Cr (VI) ion (%) is given by Eqs. (14) and (15):

$$m_{total} = \frac{C_0 Q t_{total}}{1000} \tag{14}$$

$$R = \frac{q_{total}}{m_{total}} \times 100 \tag{15}$$

where m is the mass of the adsorbent (g).

The equilibrium adsorption capacity, q_e (mg/g), and the equilibrium concentration of Cr (VI), C_e (mg/l), can be obtained from the following equations, respectively:

$$q_e = \frac{q_{total}}{m} \tag{16}$$

$$C_e = \frac{m_{total} - q_{total}}{V_{eff}} \times 1000 \tag{17}$$

The mass transfer zone (MTZ) is the region of the bed where most of the adsorption occurs and it moves up the column bed in which the adsorbate concentration changes from C/C_0 = 0.05 to 0.95. The value of MTZ can be found from:

$$MTZ = L\frac{t_e - t_b}{t_e} \tag{18}$$

where L is the bed height (cm), t_b the time required to reach the breakthrough point (min) and t_e the time required to reach the exhaust point (min).

The experimental adsorption breakthrough curves obtained from the laboratory setup were applied to the proposed model and simulate the profile of adsorption. In this study, two different models were used to fit the data obtained from the fixed-bed experiments. The Thomas model was applied to predict the breakthrough curve and to determine the operational parameters for maximum adsorption capacity at (mg/g) and the Thomas rate constant K_T (ml mg^{-1} min^{-1}), assuming second-order reversible reaction kinetics and Langmuir isotherm. The nonlinear of the Thomas model can be expressed as [17]:

$$\frac{C_t}{C_0} = \frac{1}{1+\exp\left(\frac{K_T}{Q}\left(q_T m - C_0 V\right)\right)} \tag{19}$$

where C_o is the feed concentration in mg/L, C_t the effluent concentration in mg/L, Q the flow rate in mL/min, V the volume treated in L, and m the adsorbent mass in g.

Yan developed a model to describe the adsorption breakthrough curve of the fixed-bed column. This model is considered as an empirical equation and use of the model

minimizes the error resulting from the use of the Thomas model, especially at lower or higher time periods of the breakthrough curve [18]. For a single component, the equation is:

$$\frac{C_t}{C_0} = 1 - \frac{1}{\left(\frac{QC_0t}{q_Y m}\right)^a} \quad (20)$$

where q_Y is the maximum adsorption capacity (mg/g) of adsorbent estimated by the Yan model and a constant coefficient.

3. Results and discussion

3.1. Batch adsorption studies

3.1.1. Effect of impregnation ratio of H_3PO_4 on Cr (VI) removal

Phosphoric acid is an effective activating agent for the preparation of ACs, its impregnation ratio to feedstock has been proven to have a significant effect on the porosity development [19]. In this study, the effects of the AC samples prepared with a different impregnation ratio of H_3PO_4 to municipal sewage sludge and pH on Cr (VI) removal from aqueous solution were examined and is shown in Fig. 1. As shown in Fig. 1, the Cr (VI) removal is maximum at pH 3 and increases with an increase in the impregnation ratio from 52.48 to 73.78% and then with an increase in the impregnation ratio to 3.5 g/g, it reduces to 65.36%. The reasons for this could be related to the texture characteristics of AC prepared with a different impregnation ratio chemical agent and precursor. The *general trend* in most studies revealed that the surface area of the AC increases with increasing impregnation ratios and high impregnation ratios lead to a reduction in pore volume and surface area [20], indicating the destruction of the micropores by collapsing due to the weakness of pore walls after intensive dehydration. The highest adsorption capacity was obtained for the AC sample with an impregnation ratio of 2.5 g/g and arAC sample. This means that much of the inorganic content was removed from the AC structure by acid and base refluxing, resulting in a dramatic increase in the BET surface area of 10.15 m^2/g to 472 m^2/g and mesopore volume from 0.055 to 0.446 cm^3/g. Thus, a remarkable improvement in the BET surface area and mesopore volume caused the higher Cr (VI) removal efficiency in the post-treated sample. According to the literature, mesopore has a major role in trapping large molecules of Cr (VI) [19].

3.1.2. Effect of solution pH

The pH of the aqueous phase is one of the important factors which have an effect on the adsorption capacity of the AC and also the Cr (VI) removal from solution. It has an influence on the surface charge of adsorbent and the degree of ionization and speciation of the Cr (VI) in solution [15]. Owing to this factor, its effect was investigated in the range of 2–7 and is shown in Fig. 2. As can be seen from Fig. 2, the maximum adsorption capacity of Cr (VI) was achieved at pH 3, which was about 10 mg/g and it was reduced with increasing pH. The results showed that a better Cr (VI) adsorption was yielding at low pH as observed by another researcher. Karthikeyan et al. [16] conducted the Cr (VI) adsorption with sawdust AC at the pH in the range of 1–10. Their results showed that Cr(VI) removal was pH dependent and the maximum removal efficiency was attained at pH 2. The influence of pH on Cr (VI) adsorption can be explained as follows: the main chromium hexavalent species at pH 1–6 are bichromate ($HCrO_4^-$) and dichromate ($Cr_2O_7^{2-}$) and in the neutral pH nearly all Cr is $HCrO_4^-$ or chromate (CrO_4^{2-}) while in the value above pH 7, the dominant form is CrO_4^{2-} [21]. In addition, in the acidic environment, the functional groups on the surface of the AC are protonated to a high extent which can be stated as:

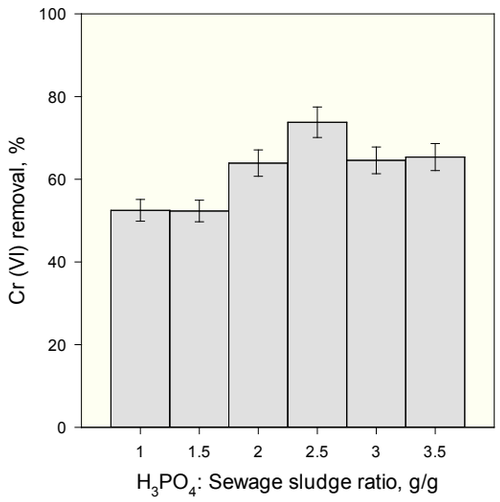

Fig. 1. Effect of different impregnation ratio of H_3PO_4 on Cr (VI) adsorption at Cr (VI) concentration of 50 mg/l, temperature of 25°C, contact time of 120 min and pH 3 and 7.

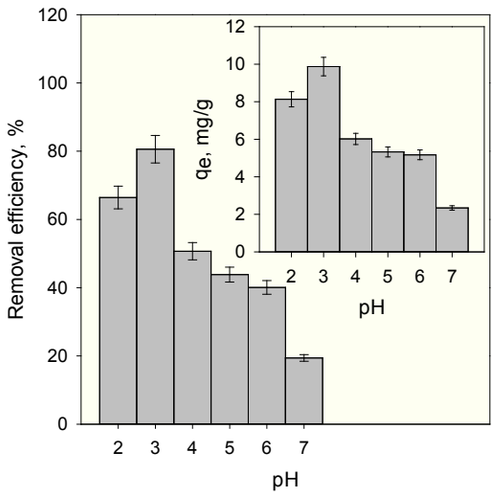

Fig. 2.Effect of pH on Cr (VI) adsorption onto $AC_{HP2.5}$ at Cr (VI) concentration of 50 mg/l, temperature of 25°C and contact time of 120 min.

$$AC\text{-}OH_2^+ \leftrightarrow AC(OH) + H^+ \quad (21)$$

$$AC(OH) \leftrightarrow AC\text{-}O^- + H^+ \quad (22)$$

Actually, the maximum Cr (VI) adsorption capacities at pH lower than 3 are related to the strong electrostatic attraction between protonated carbon surface and anionic species chromate ions from the solution which caused promotion of Cr (VI) adsorption [22]. The decrease of Cr (VI) adsorption at pH higher than 7 is attributed to $Cr_2O_7^{2-}$ and also the functional groups on the AC surface carrying negatively charged species which tends to repulse electrostatic interactions, leading to weak bonding of negative Cr formed onto the AC surface, resulting in reduction of Cr (VI) removal [23]. As aforementioned, the maximum adsorption capacity of Cr(VI) oxyanion by ACs at pH 2 can be explained by species of chromium and the ACs adsorbent surface. In fact, a mechanism of electrostatic adsorption of Cr (VI) oxyanion suggested that there is a strong electrostatic force of attraction between the $HCrO_4^-$ species with protonated active site $AC\text{-}OH_2^+$ of adsorbent surface in acidic condition as:

$$AC - OH_2^+ + HCrO_4^- \rightarrow ACHCrO_4 + H_2O, at\ pH2 \quad (23)$$

However, the electrostatic force of attraction between Cr (VI) oxyanion and the surface of ACs decreases with the pH increasing in the adsorption process. Thus, the adsorption increases with the Cr (VI) solution pH decreasing when the Cr (VI) solution is acidic.

3.1.3. Effect of adsorbent dosage

In order to select the most effective adsorbent dose for removal of Cr (VI) from aqueous solution, the influence of different doses of AC (2, 3, 4 and 5 g/l) was examined. Their results are presented in Fig. 3 and indicate that the Cr (VI) removal is a function of AC dosage. From Fig. 3, it is obvious that the percentage removal of Cr (VI) rose from 68% to 75% with increasing the adsorbent dose from 2 to 5 g/l. The phenomenon of improving metal ion adsorption is attributed to increasing of the type and the number of available binding sites on the total surface area for complexion, which result in more Cr (VI) being attached to the surface of adsorbent [24]. However, with increment adsorbent dose, Cr (VI) adsorption capacity decreased from 17.1 mg/g to 7.5 mg/g, as shown in Fig. 3. It can be due to the splitting influence of the concentration gradient between adsorbate and adsorbent with increased AC dosage and high density of adsorbent particles or inter-particle interaction, such as aggregation [25]. Since the uptake capacity is measured by a unit weight of adsorbent, from an economic standpoint, it is considered as a parameter to determine the most effective adsorbent dose. Therefore, the optimum adsorbent dose was chosen 0.4 g/100 ml for further experiments in this study.

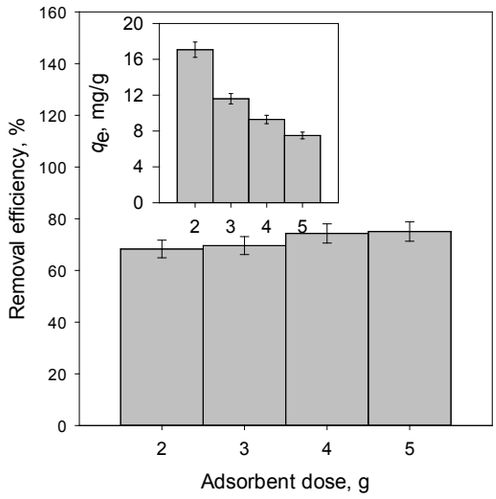

Fig. 3. Effect of adsorbent dosage on Cr(VI) adsorption onto $AC_{HP2.5}$ at Cr (VI) concentration of 50 mg/l, temperature of 25°C, contact time of 120 min and pH 3.

3.1.4. Effect of initial concentration

The investigation of initial metal concentration provides the necessary driving force to overcome all mass transfer resistance for metal ions between the solution and solid phase [26]. The effect of initial Cr (VI) ion concentration on adsorption onto AC samples (ACHP 2.5 and haAC) was studied in the range of 10–110 (figure not shown). Results showed that the amount of Cr (VI) adsorbed onto ACHP2.5 and haAC increased from 1.8 to 9.7 mg/g and 4.5 mg/g to 23.5 mg/g, respectively, by increasing initial Cr (VI) concentration from 10 to 110 mg/l. These trends can be explained by the fact that the driving force overcomes mass transfer resistances of metal ions between the solution and available surface active sites by increasing initial Cr (VI) concentration. The percentage removal decreased with increasing initial Cr (VI) concentration. In fact, all adsorbents have a limited number of active sites that become saturated at the higher concentration and lead to decrease in the percentage of removal efficiency [27]. However, the uptake capacity of haAC was greater than that of ACHP 2.5. This is due to that a higher BET surface area and uniform mesoporous pore structure allows the highly accessible pore surface areas.

3.1.5. Adsorption isotherms

Adsorption isotherms are crucial to explain the adsorption mechanism of adsorbate onto adsorbent surfaces [28]. The Langmuir and Freundlich models are frequently employed as adsorption isotherm models to investigate the relationship between the adsorption capacity and the equilibrium concentration. In other words, these isotherms depend on the magnitude of solute adsorbed at equilibrium per weight of adsorbent [11]. In the current study, both models were used to explain the adsorption behavior of Cr (VI) for $AC_{HP2.5}$ and haAC samples as are presented in Fig. 4. The constant parameters of these isotherms, evaluated from the nonlinear plot, are given in Table 3. The correlation coefficient value obtained from the Langmuir models was higher (R^2> 98) than Freundlich model. It can be concluded that Langmuir isotherm can describe well the Cr (VI) adsorption

in mixed sorbate-sorbent systems. From Table 3, the q_m of haAC sample was 31.7 mg/g which is higher than the q_m of $AC_{HP2.5}$ sample, 12.8 mg/g. The difference in adsorption capacity of the ACs for Cr (VI) removal may be related to BET surface area, structure properties and distribution surface functional groups [26]. For example, the haAC sample has a remarkably higher surface area and mesopore volume compared to $AC_{HP2.5}$ sample, resulting in greater adsorption capacity.

3.1.6 Adsorption kinetics

The study of adsorption kinetics gives valuable information about the reaction pathways and the mechanism of adsorption operations such as mass transfer, the uptake rate of adsorbate onto the adsorbent and this rate controls the residence time of adsorbate at the solid-solution interface [27]. Many kinetic models have been used to fit the adsorption process. The pseudo-first-order model [29], pseudo- second-order model [30] are mostly applied to survey the adsorption kinetics. Adsorption kinetics of Cr (VI) onto ACHP2.5 and haAC samples were examined with pseudo-first-order and pseudo- second-order models. The linear plots of these kinetic models were presented in Fig.5. It is obvious that linear plots of pseudo-second-order plots fitted the experimental data very well while pseudo-first-order kinetic model does not fit the experimental data (not shown as a figure). Kinetic constants determined from linear plots of both models and correlation coefficient values are summarized in Table 4. It can be seen from Table 4 that the correlation coefficients of pseudo-first-order model show the weak correlation of Cr(VI) adsorption onto the AC. The pseudo-second-order model indicates high correlation coefficient value which successfully expressed the kinetic process of Cr (VI) adsorption. Moreover, q_e values calculated from predicted pseudo-second-order model are nearly at experimental q_e values. Finally, it can be concluded that the adsorption of Cr (VI) with AC based sewage sludge is chemisorption because pseudo-second-order kinetic model proposes that adsorption phenomenon involves chemical adsorp-

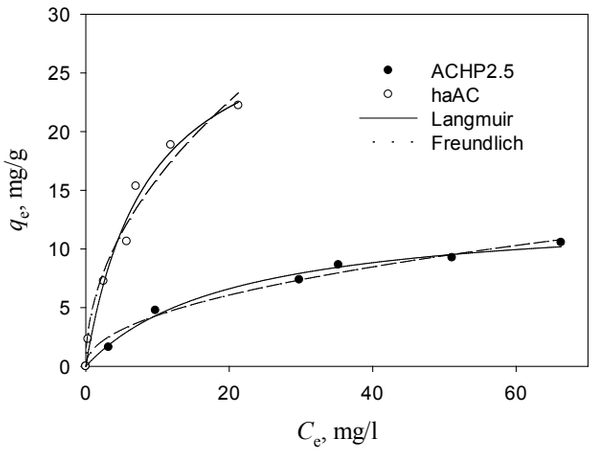

Fig. 4. Langmuir and Freundlich isotherms for Cr (VI) adsorption onto $AC_{HP2.5}$ and haAC samples at dosage of 0.4g/100 ml, temperature 25°C, agitation rate of 150 rpm, contact time of 120 min and pH 3.

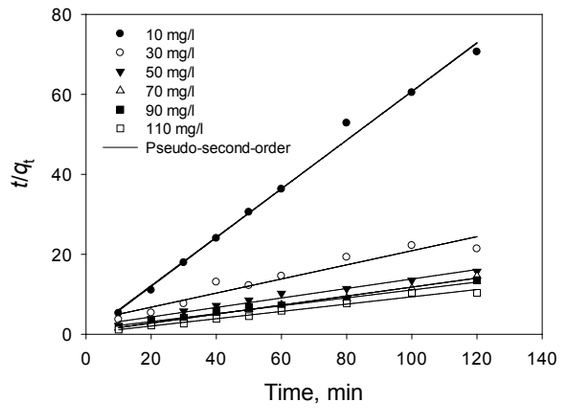

(a)

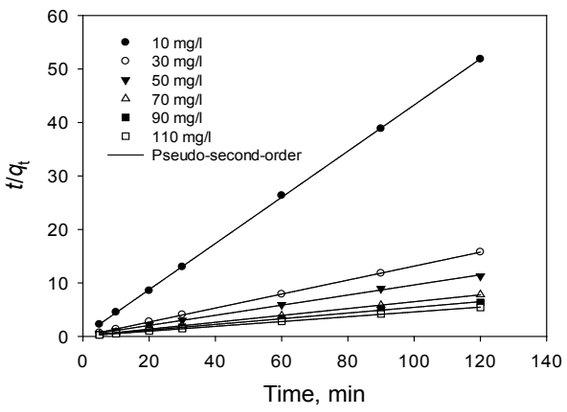

(b)

Fig. 5. Pseudo-second-order kinetic model for Cr (VI) adsorption onto (a) $AC_{HP2.5 and}$ (b) haACat dose of 0.4 g/100 ml, temperature of 25°C and pH 3.

Table 3
Langmuir and Freundlich model parameters for $AC_{HP2.5}$ and haAC

Sample	Langmuir isotherm			Freundlich isotherm		
	b, l/mg	q_m, mg/l	R^2	K_f mg/g(L/mg)^n	n	R^2
$AC_{HP2.5}$	0.0613	12.803	0.9900	1.93	2.42	0.9800
haAC	0.1148	31.72	0.9800	5.10	2.00	0.9200

Table 4
Pseudo-first-order and pseudo-second-order kinetic models for different initial concentration of Cr (VI) onto $AC_{HP2.5}$ and haAC

Sample	Metal Con., mg/l	q_{exp}, mg/g	Pseudo-first-order			Pseudo-second-order		
			k_1, min^{-1}	q_{e1}, mg/g	R^2	k_2, g/mg min	q_{e2}, mg/g	R^2
$AC_{HP2.5}$	10	1.7	0.006	4.59	0.023	0.46	1.65	0.99
	30	5.62	0.011	3.26	0.72	0.020	5.67	0.93
	50	7.65	0.008	3.60	0.28	0.014	8.43	0.98
	70	8.24	0.01	4.40	0.19	0.025	8.88	0.99
	90	8.87	0.014	3.85	0.69	0.012	10.12	0.98
	110	11.61	0.013	4.17	0.53	0.033	10.96	0.98
haAC	10	2.33	0.039	4.30	0.1	1.510	2.32	0.99
	30	7.62	0.032	5.45	0.1	0.226	7.63	0.99
	50	10.64	0.01	1.60	0.1	0.056	10.53	0.99
	70	15.35	0.01	1.60	0.1	0.057	15.63	0.99
	90	18.86	0.04	6.78	0.1	0.025	18.87	0.99
	110	22.23	0.02	4.10	0.4	0.026	22.22	0.99

tion mechanism. In this regard, several studies have been reported that used the pseudo-second-order kinetic model to describe Cr (VI) adsorption [26].

3.1.7. Effect of temperature and thermodynamic parameters

Temperature is one of the parameters that have an evident influence on the adsorption of Cr (VI) onto AC samples. The Arrhenius plot, using pseudo-second-order kinetic data, and Van't Hoff plot is shown in Fig. 6. The thermodynamic parameters including Gibbs free energy change (ΔG°), enthalpy change (ΔH°) and entropy change (ΔS°) are given in Table 5. ΔH° is associated with the energy released when the adsorbate and adsorbent are linked. The negative ΔH° value confirms that the adsorption nature of Cr (VI) onto $AC_{HP2.5}$ is an exothermic process, which can be due to different functional groups and adsorption sites on the AC surface prepared from sewage sludge. Positive ΔH° demonstrates that the adsorption of Cr (VI) onto haAC is endothermic, which is proved by an increase in the adsorption of Cr (VI) with temperature. The low value of ΔH° for both samples suggests that the physical adsorption may be responsible for Cr (VI) removal from aqueous solution in which the forces involved in adsorption phenomenon are weak, this is according to thumb law which states the physical adsorption process that can be occurred in ΔH° value is between 2–40 kJ/mol [31]. The negative value of ΔS° reveals a decrease in randomness at the solid/liquid interface during the adsorption of Cr (VI) onto $AC_{HP2.5}$. While the positive value of ΔS° explained that the degree of randomness increased at the solid/liquid interface during the adsorption of Cr (VI) onto the haAC. This is probably due to some structural changes in the adsorbent and adsorbate as immobilization Cr (VI) ions induced onto adsorbent surface compared with a solution [32]. For $AC_{HP2.5}$ sample, the values of Gibbs free energy were positive at all of the tested temperatures, indicating that the adsorption of Cr (VI) onto AC was thermodynamically nonspontaneous in nature. Similarly, the increase in the positive values of ΔG° with

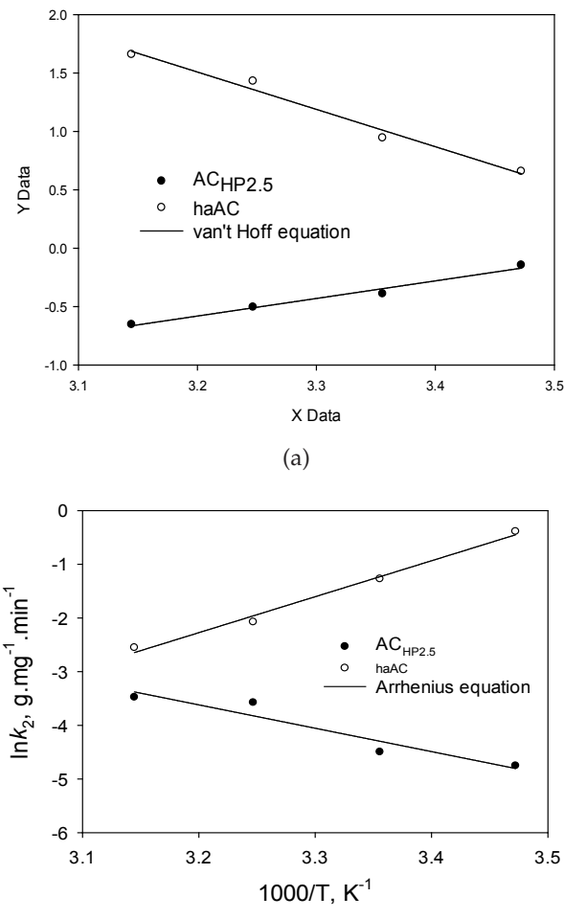

Fig. 6. (a) Van't Hoff and (b) Arrhenius plots of Cr (VI) adsorption onto $AC_{HP2.5}$ and haAC at adsorbent dose of 0.4 g/100 ml, pH 3.0, initial concentration of 50 mg/L, contact time of 120 min and agitation rate of 150 rpm.

Table 5
Thermodynamic parameters of Cr (VI) adsorption on $AC_{HP2.5}$ and haAC at initial metal concentration of 50 mg/l and at different temperatures

AC type	ΔH°, kJ/mol	ΔS°, J/mol·K	ΔG°, kJ/mol				R^2	*Ea*, kJ/mol	R^2
			288 K	298 K	308 K	318 K			
$AC_{HP2.5}$	–16.63	–61.94	1.21	1.83	2.45	3.07	0.9818	36.20	0.9097
haAC	26.58	97.61	–1.53	–2.50	–3.48	–4.46	0.9829	–55.68	0.9900

an increase in temperature explains a decrease infeasibility of nonspontaneous adsorption at a higher temperature. So the adsorption process at a lower temperature is more feasible [33]. However, for haAC sample, the ΔG° values were negative at all of the tested temperatures, implying that the adsorption of Cr (VI) onto haAC was thermodynamically favorable and spontaneous in nature. Therefore, the ΔG° results suggested that the adsorption affinity of Cr (VI) onto ha AC was stronger that onto $AC_{HP2.5}$.

3.2. Adsorption Cr (VI) in fixed-bed column and breakthrough analysis

3.2.1. Effect of feed concentration Cr (VI)

The effect of the influent concentration on the adsorption Cr (VI) was investigated using various Cr (VI) concentrations of 20, 40 and 60 mg/l at a constant bed height of 4 cm and flow rate of 1 ml/min. The effect of influent concentration on the shape and appearance of the breakthrough curves and the column adsorption parameters was considered. The results are presented in Fig. 7a and Table 6. Results showed that the breakthrough curve was rather steep, time of breakthrough (t_b at $C_t/C_o = 0.05$) and column exhaustion (t_e at $C_t/C_o = 0.95$) was very fast and greater uptake capacity obtained at 60 mg/l, due to that higher concentration creates a driving force to an enhanced dispersion of metal ion along the column. As the breakthrough analysis is shown in Table 6, with increase in the Cr (VI) concentration at 20, 40 and 60 mg/l, the removal was 56, 63 and 77%, respectively. This trend is due to the decrease in the total passed the volume of metal solution through the column with the increase in the influent metal concentration until the column reaches to exhaustion time [34,35].

3.2.2. Effect of flow rate

For continuous treatment of wastewater on an industrial scale, the flow rate is an important parameter in estimating the performance of adsorbent. The breakthrough curves for Cr (VI) adsorption on $S_{2.5}$ at different flow rates of 0.5, 1 and 1.5 ml/min through a 4 cm column bed height and influent concentration of 40 mg/l are shown in Fig. 7b and the breakthrough analysis presented in Table 6. These results reveal that a decreased breakthrough time (t_b) and exhaustion time (t_e) was observed with the increase in flow rate from 0.5 to 1.5 ml/min. The analysis of the breakthrough curve showed that the increase in column flow rate from 0.5 to 1.5 ml/min resulted in a decrease in

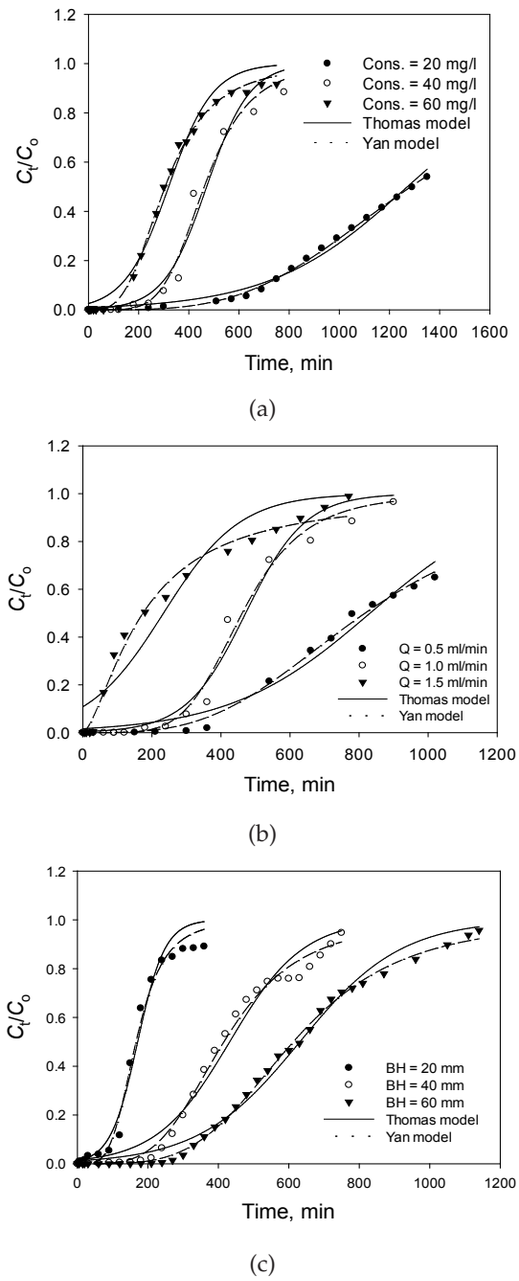

Fig. 7. Experimental breakthrough curve at different (a) inlet Cr(VI) concentration (b) flow rates and (c) and bed heights for Cr (VI) removal using $AC_{HP2.5}$.

Table 6
The breakthrough parameters and Thomas and Yan models of Cr (VI)adsorption on $AC_{HP2.5}$ in a fixed-bed column

Type of AC	Column condition			Breakthrough analysis					Thomas model			Yan model		
	Cons., mg/l	BH, mm	Q, ml/min	q_e, mg/g	R, %	C_e, mg/l	MTZ, cm	t_e, min	q_T, mg/g	$K_T \times 10^4$	R^2	q_Y, mg/g	a	R^2
Synthetic wastewater sample:														
$AC_{HP2.5}$	20	40	1.0	10.98	56.00	7.59	2.87	2020	12.6	0.35	0.99	11.83	4.64	0.99
	40	40	1.0	9.50	63.00	9.30	2.80	780	9.2	0.38	0.98	8.93	3.92	0.99
	60	40	1.0	11.14	77.00	13.70	3.00	490	10.83	0.38	0.99	11.85	3.27	0.99
	40	20	1.0	17.63	61.78	15.29	1.44	750	16.43	0.34	0.98	15.62	3.34	0.99
	40	60	1.0	8.00	54.54	18.81	4.38	1110	76.42	0.27	0.98	8.20	4.00	0.99
	40	40	0.5	11.60	31.42	27.43	3.62	3840	10.52	0.40	0.96	11.08	2.37	0.99
	40	40	1.5	7.55	37.35	25.06	3.83	701	8.12	0.36	0.96	7.45	2.52	0.99
arAC	40	20	1.0	12.70	46.00	29.00	1.90	780	13.71	0.35	0.96	12.92	3.22	0.99
brAC				31.10	79.00	8.22	2.75	800	30.15	0.54	0.98	31.00	4. 41	0.99
haAC				94.54	90.00	5.22	1.90	1245	95.11	0.74	0.99	95.89	5.57	0.99
bsAC				18.26	56.34	15.29	1.44	990	18.12	0.38	0.97	18.61	2.84	0.99
Electroplating wastewater sample:														
$AC_{HP2.5}$	110	20	1.0	7.20	30.66	103.00	1.75	180	6.00	8.96	0.98	5.95	121.8	0.99
haAC				33.86	66.00	104.84	1.83	480	34.12	2.33	0.99	34.99	306.14	0.99

BH: bed height (mm); Q: flow rate (ml/min); Cons.: inlet concentration (mg/l); q_e: adsorption capacity (mg/g); R: percentage removal; C_e: equilibrium concentration (mg/l); MTZ: mass transfer zone (mm); t_e: exhausting time (min); c k_{Th}: Thomas rate constant (ml/min/mg); q_{Th}: Thomas maximum adsorption capacity (mg/g); a: Yan constant (dimensionless); q_Y: Yan maximum adsorption capacity (mg/g).

the Cr (VI) uptake capacity from 11.6 to 7.55 mg/g, due to metal ions did not have enough opportunity to link with the adsorbent surface of the AC, whereas the mass transfer zone (MTZ) values increased from 3.62 to 3.83 mm, respectively. This means that the increase in column flow rate resulted in MTZ length to a higher zone, so before reaching equilibrium metal ions are passed through the column and reduced performance of the column because of the spreading of the breakthrough curve may be caused by the MTZ limitations [36]. These results are of importance because the adsorbent bed is operational until the MTZ reaches the adsorber end.

3.2.3. Effect of bed high

The uptake of metals in the fixed-bed column is dependent on the quantity of adsorbent in the column. The bed height experiments were conducted using a fixed-bed column with AC for three different bed heights of 2, 4 and 6 cm at a constant flow rate of 1 ml/min and an influent Cr (VI) concentration of 40 mg/l. The breakthrough curves at different bed heights were shown in Fig. 7(c) and the breakthrough analysis summarized in Table 6. The observed breakthrough curve in higher column bed height has a gradual shape of the curve. By increasing bed high from 2 to 4 cm, removal of Cr (VI) increased from 61 to 63% due to the number of active sites available on the adsorbent surface because of MTZ needs more time to reach the column end and for the metal ions to have more time to be in contact with AC. But in bed height from 4 to 6 cm, removal of Cr (VI) (54%) did not show a similar trend because in bed height 6 cm, t_b increases from 780 to 1110 min, so more solution passes through the fix-bed column and the removal percentage obtained less than bed high of 2 and 4 cm.

3.3. Modeling of fix bed column

The Thomas and Yan models were applied to fit the experimental data in a fix-bed column in order to determine the rate constant, maximum uptake capacity and to predict the breakthrough curve for dynamic adsorption of Cr (VI). The breakthrough curves predicted by the Yan and Thomas models at different bed height, flow rate and inlet concentration for the removal of Cr (VI) are shown in Fig. 7a–c and constant parameters of Thomas and Yan models are listed in Table 6. The Yan model gave a good fit to the experimental data and obtained a high correlation coefficient (range of R^2= 0.9941–0.991). By comparison of uptake capacity of the experimental data with the Yan model predicted breakthrough curves is clear that Yan model fitted better than the Thomas model. However, the data in Table 6 reveal a negligible difference between the Yan model and Thomas models values of R^2 and the experimental values of uptake capacities were similar to the predicted values from both models for Cr (VI) in all operational conditions. The constant rate of the Thomas model increased with increasing inlet concentration of Cr (VI), due to the interaction between Cr (VI) and A which provides the essential driving force to overcome the resistances to the mass transfer of Cr VI) between the aqueous solution and the AC adsorbent. However, the values of K_{th} was not influenced much by flow rate and increased with increasing bed height, indicating the kinetic in the fixed-bed column is controlled by external mass transfer.

3.4. Effect of acid- and base-refluxed AC on adsorption of Cr (VI) in a fixed-bed column

In order to increase percentage removal and surface area AC-based sewage sludge, the fix-bed column carried out for different AC-based sewage sludge which reflexed with acid and base leaching methodology. The experiments results of the breakthrough analysis and constant parameters of Thomas and Yan models forbs AC, arAC, brAC and haAC samples at a bed height of 20 mm, the flow rate of 1 ml/min and an influent Cr (VI) concentration of 40 mg/l are summarized in Table 6. The percentage removal of Cr (VI) increases from 61.78 to 79.00 and uptake capacity values increased from 17.63 to 31.10 mg/g for $AC_{HP2.5}$ and arAC, respectively. This increase is due to a decrease in mineral content and silica precursor, which was ultimately led to an increase in porosity and BET surface area of AC. The percentage removal of Cr (VI) by AC treated with HF improved significantly compared to other treatment methods. The percentage removal of Cr (VI) increased from 61.78 to 90.00 and uptake capacity values increased from 17.63 to 94.54 mg/g for $AC_{HP2.5}$ and haAC, respectively. It can be explained that the pore size treated with HF is mesoporous. On the other hand, ionic radius of Cr (VI) is large, therefore, this AC treated with HCl-HF better able to remove chromium (VI) from aqueous solution. The surface area of the bsAC obtained from two stages (635 m^2/g) process was found to be much higher than those AC obtained from the one stage process. However, the average pore diameter and mesoporosity percent were less which leads to decrease in percentage removal and uptake capacity. This clearly demonstrates that the two stage process enhances the microporosity development. Removal percentage of Cr (VI) and uptake capacity were not changed significantly for arAC sample compared with other AC samples.

3.5. Electroplating wastewater adsorption onto AC sample

In order to survey capability of the prepared adsorbents for removal of Cr (VI) from electroplating industry wastewater, fixed-bed column experiments by $AC_{HP2.5}$ and haAC samples were conducted. The breakthrough curves predicted by the Yan and Thomas models for the removal of Cr (VI) from electroplating wastewater are shown in Fig. 8 and the breakthrough parameters for Cr (VI) removal by $AC_{HP2.5}$ and haAC are summarized in Table 6. Results showed that fixed-bed column indicated that haAC exhibited a high removal capacity toward Cr(VI) from electroplating wastewater, which contains the highest concentration TDS and EC (Table 1) and may interfere adsorption of Cr (VI). The removal of Cr (VI) by $AC_{HP2.5}$ was weakened in the presence of other impurities, as a result of the less BET surface area and active sites of the adsorbent surface. Overall, as prepared haAC were potential adsorbent for the removal of Cr (VI) from wastewater.

3.6. Desorption

The regeneration of the adsorbent is important, especially if the adsorption is to be employed for treatment of industrial wastewater because it leads to reuse adsorbent and decreasing the cost of adsorption production. The aim

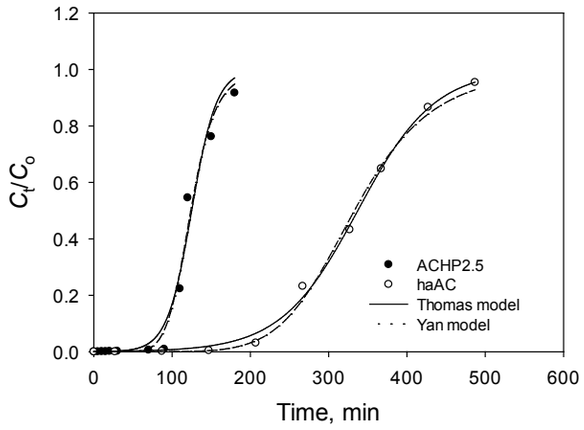

Fig. 8. Removal of Cr (VI) ions from electroplating wastewater using (a) $AC_{HP2.5}$, (b) haAC at pH = 3 and room temperature.

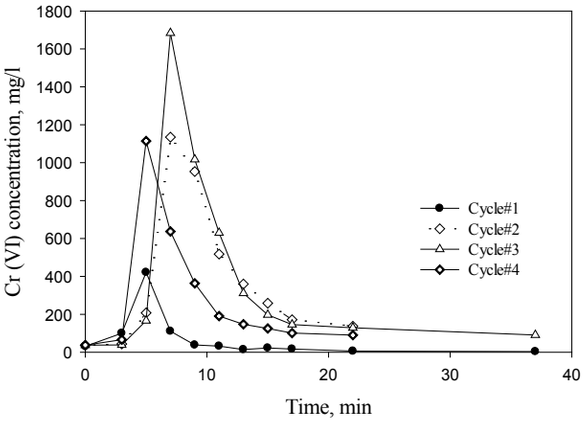

Fig. 9. Desorption cycles on activated carbon.

is to remove the loaded Cr (VI) from the fixed-bed adsorbent in the smallest possible volume of an eluting solution. The sorption-desorption experiments were studied using 0.5M NaOH solution under identical conditions of the flow rate of 1 ml/min, the bed height of 40 mm and inlet Cr (VI) concentration of 50 mgl/l. In every cycle, the loading was considered complete when the Cr (VI) concentration in the effluent was equal to inlet Cr (VI) concentration. The results of the desorption tests are presented in Fig. 5. The recovery percentage in three cycles changed from 60% to 40%. This drop may be due to the fact that chemisorption mechanism was involved on the surface and Cr (VI) was less removed in the pores of haAC. These results indicate that the recovery percentage of Cr (VI) was unsatisfactory. Therefore, the effect of the different leaching agent, temperature, and leaching rate on the desorption concentration of Cr (VI) from AC derived sewage sludge should be investigated.

3.7. Comparison with other AC

The maximum adsorption capacity of Cr (VI) onto AC samples was compared with other AC which was produced

Table 7
Comparison of maximum adsorption capacities of various AC adsorbents for Cr (VI) removal

Adsorbent	pH	Temperature, °C	q_m, mg/g	Ref.
Commercial AC	6	25	4.7	[37]
Commercial AC oxidized with H_2SO_4	6	25	8.9	
Commercial AC oxidized with HNO_3	6	25	10.4	
AC-based fabric cloth	2	25	21.8	[39]
Bio-char	2	25	9.5	
Bio-char	2	25	10	
AC-based agricultural waste	2	25	11.5	
Sewage sludge AC	3	25	15.4	[40]
AC-biomass	1.5	25	9.97	[26]
Tamarind wood AC	5.6	50	28.01	[41]
Waste tires AC	2	22	29.93	[38]
Sawdust AC	2	22	24.65	
Palm shell AC	4	25	12.6	[23]
PEI/palm shell AC	4	25	20.5	
$AC_{HP2.5}$	3	25	12.8	In this study
haAC	3	25	31.7	

from different precursor materials and summarized in Table 7. It can be seen that Cr (VI) maximum adsorption capacity of the $AC_{HP2.5}$ sample (12.8 mg/g) is comparable to the adsorption capacity of commercial AC (9.97 mg/g and 10.4 mg/g) [26,37] reported in the literature. However, haAC sample (31.7 mg/g) has sufficiently high Cr (VI) adsorption capacity compared to palm shell (12.6 mg/g) [23], sawdust (24.6 mg/g) [38], waste tires (29.9 mg/g) [38], coconut shell (11.5 mg/g) [39] and also sewage sludge AC (15.4 mg/g) [40]. Based on the literature, the initial carbon content of feedstock, activation process and pore development are responsible for the adsorption capacity of metal ions [16]. For example, in this study, the haAC-based sewage sludge has higher Cr(VI) adsorption capacity (two times more) than that obtained by Rozada et al. [40]. It can be explained the use mild acid leaching and in their refluxing treatment processes on pyrolyzed AC in order to remove silica and all the metal impurities.

4. Conclusions

The potential of Cr (VI) removal from aqueous solution onto AC samples was investigated in a different condition of pH, initial Cr (VI) concentration, adsorbent dosage, contact time and temperature. The adsorption experiments were conducted in batch and fixed-bed systems. The maximum adsorption capacity of Cr (VI) was obtained at pH 3. The adsorption behavior of Cr (VI) onto AC samples was fitted by Langmuir and Freundlich models and maximum equilibrium adsorption capacity of 12.80 and 31.7 mg/g were obtained for $AC_{HP2.5}$ and haAC samples, respectively, which indicated washing refluxing sludge AC with HCl and NaOH notably improved Cr (VI) removal efficiency. The pseudo-first-order and the pseudo-second-order kinetic model were applied to explain the synthetics of Cr (VI) adsorption. Taking into consideration the activation energy and enthalpy, the main adsorption mechanisms for Cr (VI) onto ST and $S_{2.5}$ samples were chemisorption and physical adsorption, respectively. The results of thermodynamic studies show that Cr (VI) adsorption process is spontaneous and upgraded by reducing the temperature from 15 to 45°C. In the continuous operation, effects on the breakthrough curve of bed height, flow rate and initial ion concentration were investigated, while the experimental adsorption capacity reached to 94.54 mg/g. The Yan model predicted the maximum adsorption capacity better than the Thomas model. The adsorption–desorption experiments by NTAC showed that the adsorption capacity decreases from 15.6 to 8.34 mg/g. After four cycles, demonstrating a good regeneration capacity of the adsorbent for treating wastewater containing hexavalent chromium ions. Finally, we found out that AC derived sewage sludge If is rinsed with acid is a good adsorbent for hexavalent chromium ion removal (by 96%) from electroplate wastewater.

Acknowledgments

The authors wish to thank the Ministry of Science, Research and Technology of Iran and the Faculty of Natural Resources of the Tarbiat Modares University (TMU) for their financial support, from which funding and a research grant made this study possible. Also, we would like to thank Mrs. Haghdoust (Technical Assistant of Environmental Laboratory at TMU) and Engineer M. Aghajani for their assistance.

References

[1] S.B. Lalvani, T. Wiltowski, A. Hübner, A. Weston, N. Mandich, Removal of hexavalent chromium and metal cations by a selective and novel carbon adsorbent, Carbon, 36 (1998) 1219–1226.
[2] Z. Aksu, T. Kutsal, S. Gün, N. Haciosmanoglu, M. Gholaminejad, Investigation of biosorption of Cu (II), Ni (II) and Cr (VI) ions to activated sludge bacteria, Environmen. Technol., 12 (1991) 915–921.
[3] F.-S. Zhang, J.O. Nriagu, H. Itoh, Mercury removal from water using activated carbons derived from organic sewage sludge, Water Res., 39 (2005) 389–395.
[4] E. Padilla-Ortega, R. Leyva-Ramos, J.V. Flores-Cano, Binary adsorption of heavy metals from aqueous solution onto natural clays, Chem. Eng. J., 225 (2013) 535–546.
[5] A. Stafiej, K. Pyrzynska, Adsorption of heavy metal ions with carbon nanotubes, Separ. Purif. Technol., 58 (2007) 49–52.
[6] T. Motsi, N.A. Rowson, M.J.H. Simmons, Adsorption of heavy metals from acid mine drainage by natural zeolite, Int. J. Miner. Process., 92 (2009) 42–48.
[7] K.M. Smith, G.D. Fowler, S. Pullket, N.J.D. Graham, Sewage sludge-based adsorbents: A review of their production, properties and use in water treatment applications, Water Res., 43 (2009) 2569–2594.
[8] APHA, Standard methods for the examination of water and wastewater, 20th ed., Washington DC, 1998.
[9] Z. Aliakbari, H. Younesi, A.A. Ghoreyshi, N. Bahramifar, A. Heidari, Production and characterization of sewage-sludge based activated carbons under different post-activation conditions, Waste Biomass Valorization, (2017) 1–13 (In Press).

[10] M. Bansal, D. Singh, V.K. Garg, A comparative study for the removal of hexavalent chromium from aqueous solution by agriculture wastes' carbons, J. Hazard. Mater., 171 (2009) 83–92.
[11] T.W. Webi, R.K. Chakravort, Pore and solid diffusion models for fixed-bed adsorbers, AIChE J., 20 (1974) 228–238.
[12] F. Bouhamed, Z. Elouear, J. Bouzid, Adsorptive removal of copper(II) from aqueous solutions on activated carbon prepared from Tunisian date stones: Equilibrium, kinetics and thermodynamics, J. Taiwan Inst. Chem. Eng., 43 (2012) 741–749.
[13] K. Wilson, H. Yang, C.W. Seo, W.E. Marshall, Select metal adsorption by activated carbon made from peanut shells, Bioresour. Technol., 97 (2006) 2266–2270.
[14] D. Mohan, S. Rajput, V.K. Singh, P.H. Steele, C.U. Pittman Jr, Modeling and evaluation of chromium remediation from water using low cost bio-char, a green adsorbent, J. Hazard. Mater., 188 (2011) 319–333.
[15] I. Kula, M. Uğurlu, H. Karaoğlu, A. Çelik, Adsorption of Cd(II) ions from aqueous solutions using activated carbon prepared from olive stone by $ZnCl_2$ activation, Bioresour. Technol., 99 (2008) 492–501.
[16] T. Karthikeyan, S. Rajgopal, L.R. Miranda, Chromium(VI) adsorption from aqueous solution by Hevea Brasilinesis sawdust activated carbon, J. Hazard. Mater., 124 (2005) 192–199.
[17] H.C. Thomas, Heterogeneous ion exchange in a flowing system, J. Amer. Chem. Soc., 66 (1944) 1664–1666.
[18] G. Yan, Viraraghavan, T. Viraraghavan, M. Chen, A new model for heavy metal removal in a biosorption column, Adsorp. Sci. Technol., 19 (2001) 25–43.
[19] M.A. Nahil, P.T. Williams, Pore characteristics of activated carbons from the phosphoric acid chemical activation of cotton stalks, Biomass Bioenergy, 37 (2012) 142–149.
[20] V. Fierro, V. Torné-Fernández, A. Celzard, Methodical study of the chemical activation of Kraft lignin with KOH and NaOH, Micropor. Mesopor. Mater., 101 (2007) 419–431.
[21] M. Bagheri, H. Younesi, S. Hajati, S.M. Borghei, Application of chitosan-citric acid nanoparticles for removal of chromium (VI), Int. J. Biol. Macromol., 80 (2015) 431–444.
[22] D. Duranoğlu, A.W. Trochimczuk, U. Beker, Kinetics and thermodynamics of hexavalent chromium adsorption onto activated carbon derived from acrylonitrile-divinylbenzene copolymer, Chem. Eng. J., 187 (2012) 193–202.
[23] M. Owlad, M.K. Aroua, W.M.A. Wan Daud, Hexavalent chromium adsorption on impregnated palm shell activated carbon with polyethyleneimine, Bioresour. Technol., 101 (2010) 5098–5103.
[24] C. Namasivayam, R.T. Yamuna, Adsorption of chromium (VI) by a low-cost adsorbent: Biogas residual slurry, Chemosphere, 30 (1995) 561–578.
[25] M. Amini, H. Younesi, N. Bahramifar, Biosorption of U(VI) from aqueous solution by chlorella vulgaris: equilibrium, kinetic, and thermodynamic studies, J. Environ. Eng., 139 (2013) 410–421.
[26] H. Deveci, Y. Kar, Adsorption of hexavalent chromium from aqueous solutions by bio-chars obtained during biomass pyrolysis, J. Ind. Eng. Chem., 19 (2013) 190–196.
[27] Z.A. Al-Othman, R. Ali, M. Naushad, Hexavalent chromium removal from aqueous medium by activated carbon prepared from peanut shell: Adsorption kinetics, equilibrium and thermodynamic studies, Chem. Eng. J., 184 (2012) 238–247.
[28] A.B. Albadarin, C. Mangwandi, A.a.H. Al-Muhtaseb, G.M. Walker, S.J. Allen, M.N.M. Ahmad, Kinetic and thermodynamics of chromium ions adsorption onto low-cost dolomite adsorbent, Chem. Eng. J., 179 (2012) 193–202.
[29] V.K. Singh, P.N. Tiwari, Removal and recovery of chromium (VI) from industrial waste water, J. Chem. Technol. Biotechnol., 69 (1997) 376–382.
[30] Y.S. Ho, J.F. Porter, G. McKay, Equilibrium isotherm studies for the sorption of divalent metal ions onto peat: copper, nickel and lead single component systems, Water Air Soil Pollut., 141 (2002) 1–33.
[31] I.N. Levine, Physical Chemistry, McGraw-Hill, Boston, MA, 2008.
[32] K. Li, X. Wang, Adsorptive removal of Pb (II) by activated carbon prepared from S*partina alterniflora*: Equilibrium, kinetics and thermodynamics, Bioresour. Technol., 100 (2009) 2810–2815.
[33] A. Sari, M. Tuzen, D. Citak, M. Soylak, Equilibrium, kinetic and thermodynamic studies of adsorption of Pb(II) from aqueous solution onto Turkish kaolinite clay, J. Hazard. Mater., 149 (2007) 283–291.
[34] M. Hadavifar, N. Bahramifar, H. Younesi, Q. Li, Adsorption of mercury ions from synthetic and real wastewater aqueous solution by functionalized multi-walled carbon nanotube with both amino and thiolated groups, Chem. Eng. J., 237 (2014) 217–228.
[35] A. Shahbazi, H. Younesi, A. Badiei, Batch and fixed-bed column adsorption of Cu(II), Pb(II) and Cd(II) from aqueous solution onto functionalised SBA-15 mesoporous silica, Canad. J. Chem. Eng., 91 (2013) 739–750.
[36] A. Shahbazi, H. Younesi, A. Badiei, Functionalized SBA-15 mesoporous silica by melamine-based dendrimer amines for adsorptive characteristics of Pb(II), Cu(II) and Cd(II) heavy metal ions in batch and fixed bed column, Chem. Eng. J., 168 (2011) 505–518.
[37] S. Babel, T.A. Kurniawan, Cr(VI) removal from synthetic wastewater using coconut shell charcoal and commercial activated carbon modified with oxidizing agents and/or chitosan, Chemosphere, 54 (2004) 951–967.
[38] N.K. Hamadi, X.D. Chen, M.M. Farid, M.G.Q. Lu, Adsorption kinetics for the removal of chromium(VI) from aqueous solution by adsorbents derived from used tyres and sawdust, Chem. Eng. J., 84 (2001) 95–105.
[39] D. Mohan, K.P. Singh, V.K. Singh, Removal of hexavalent chromium from aqueous solution using low-cost activated carbons derived from agricultural waste materials and activated carbon fabric cloth, Ind. Eng. Chem. Res., 44 (2005) 1027–1042.
[40] F. Rozada, M. Otero, A. Morán, A.I. García, Adsorption of heavy metals onto sewage sludge-derived materials, Bioresour. Technol., 99 (2008) 6332–6338.
[41] J. Acharya, J.N. Sahu, B.K. Sahoo, C.R. Mohanty, B.C. Meikap, Removal of chromium(VI) from wastewater by activated carbon developed from Tamarind wood activated with zinc chloride, Chem. Eng. J., 150 (2009) 25–39.